



MODELLING OF DYNAMICAL SYSTEMS WITH FRICTION BETWEEN RANDOMLY ROUGH SURFACES

Nicole Gaus^{*}, Carsten Proppe^{*} e Cédric Zaccardi^{*}

^{*} Institut für Technische Mechanik (ITM)

Karlsruher Institut für Technologie (KIT)

Kaiserstr. 10, Geb. 10.23, 76131 Karlsruhe, Germany

e-mail: proppe@kit.edu

Key words: Friction-induced vibrations, Surface Roughness, Polynomial Chaos, Non-Normal Distributions.

Parole chiave: Attrito Indotta Vibrazioni, Rugosità Superficiale, Caos Polinomiale, Distribuzioni Non-Normali.

Abstract. *Friction induced vibrations are present in many engineering systems, e.g. in brakes and cam follower systems. In these systems, self-excited oscillations may occur. Surface roughness is an important source of uncertainty in friction systems. The aim of this contribution is to study the influence of surface roughness on friction induced vibrations. To this end, a statistical analysis of measured rough surfaces is carried out in order to generate statistical representative surfaces. From the Bowden-Tabor approach, the friction coefficient of these surfaces is computed and represented by a stochastic process. As an example, the classical mass on a belt system is considered, where stick-slip vibrations occur. A stochastic process is introduced into the model and its influence on the limit cycle is studied. It is shown that the stochastic nature of the friction coefficient alters the stick-slip limit cycle.*

Sommario. *Attrito indotta vibrazioni sono presenti in molti sistemi di ingegneria, ad esempio nei freni e sistemi di punteria. In questi sistemi, possono verificarsi oscillazioni auto-eccitate. Rugosità superficiale è una causa importante d'incertezza nei sistemi di attrito. Lo scopo di questo contributo è di studiare l'influenza della rugosità superficiale su attrito indotta vibrazioni. A tal fine, l'analisi statistica delle superfici ruvide misurate è effettuata al fine di generare superfici rappresentativi statistici. Dall'approccio Bowden-Tabor, il coefficiente di attrito di queste superfici è calcolato e rappresentato da un processo stocastico. Come esempio, il moto di una massa su un nastro è considerato, in cui succedono vibrazioni di tipo aderenza-slittamento. Un processo stocastico è introdotto nel modello e la sua influenza sul ciclo limite è investigata. Si mostra che la natura stocastica del coefficiente di attrito altera il ciclo limite aderenza-slittamento.*

1 INTRODUCTION

Dry friction between rough surfaces is present in many engineering systems and noise due to friction induced self-excitation is a common problem e.g. in brake systems. It is the objective

of this contribution to study the influence of the stochastic nature of the surface heights for rough surfaces on the friction coefficient and on the limit cycle of self-excited oscillatory systems with friction. To this end, a multiscale model is established, that ranges from the stochastic description of rough surfaces to the representation of the friction coefficient as a stochastic process and the identification of its properties in order to study friction oscillators with stochastic friction coefficient. The different parts of this model are described in the following sections and some consequences of the stochastic nature of the friction coefficient for friction induced vibrations are highlighted.

2 STOCHASTIC MODELS FOR ROUGH SURFACES

From white light interferometry, statistical characteristics such as the probability density function, the correlation function and the spectral density of the surface heights can be estimated. With this information, sample surfaces can be generated by means of random field representations of the surface heights $z(\mathbf{x}, \theta)$, where \mathbf{x} denotes the spatial dependence and θ represents the random event. The following two stochastic descriptions of rough surfaces are nowadays widespread [1] and are stated here for scalar spatial dependence only:

1. A fractal approach, where $z(x, \theta)$ is represented by the Weierstrass-Mandelbrot function

$$z(x, \theta) = \sum_{j=-\infty}^{\infty} \gamma^{(D-2)j} \cos(\gamma^j x + \xi_j(\theta)), \quad (1)$$

where $1 < D < 2$ denotes the fractal dimension of the surface, $\gamma > 1$ determines the density of frequencies and the random variables $\xi_j(\theta)$ that are uniformly distributed on $[0, 2\pi]$ represent random phase shifts.

2. A Karhunen-Loève expansion

$$z(x, \theta) = E[z(x, \theta)] + \sum_{j=1}^{\infty} \sqrt{\lambda_j} \varphi_j(x) \xi_j(\theta), \quad (2)$$

where (λ_j, φ_j) are the eigenvalues and eigenvectors of the covariance function of $z(x, \theta)$. In practice, this series is truncated at a given order M . If $z(x, \theta)$ is a Gaussian random field, $\xi_j(\theta)$ will be independently distributed standard Gaussian random variables.

If the random field does not follow a Gaussian distribution, an isoprobabilistic transformation can be applied in order to transform the Gaussian field into another field which follows the given probability density function, at the price of perturbing the correlation function. Both descriptions can be generalized to vector-valued spatial dependence, cf. e.g. [2] for the Weierstrass-Mandelbrot function.

3 COMPUTATION OF THE RANDOM PRESSURE FIELD

3.1 Solution of the normal contact problem

Before discussing the stochastic normal contact problem, the normal contact of a single sample of a rough surface is studied in the following. Consider the normal contact between a flexible rough and a rigid flat surface with penetration d , cf. Figure 1. If the local interference

$$\bar{u}_z(x) = z(x) - (g_0 - d) \quad (3)$$

between the two surfaces is non-negative, the two surfaces are in contact at \mathbf{x} . The total complementary potential energy is given by the difference of the surface integrals

$$V^* = \frac{1}{2} \int_S p(x) u_z(x) dS - \int_S p(x) \bar{u}_z(x) dS, \quad (4)$$

where $p(x)$ is the contact pressure and $u_z(x)$ the displacement. Under assumption of the linear elastic half-space theory, displacement and pressure are related by the Boussinesq equation

$$u_z(x, y) = \frac{1 - \nu^2}{\pi E} \int_S \frac{p(\xi, \eta) d\xi d\eta}{\sqrt{(x - \xi)^2 + (y - \eta)^2}}, \quad (5)$$

where E denotes Young's modulus and ν Poisson's ratio. This relation is discretized on a mesh for the contact surface S ,

$$u_{z,i} = \sum_{j=1}^N B_{ij} p_j \quad (6)$$

and inserted into the discretized expression for the complementary potential energy:

$$V^* = \frac{1}{2} \sum_{i=1}^N p_i \left(\sum_{j=1}^N B_{ij} p_j \right) - \sum_{i=1}^N p_i \bar{u}_{z,i}. \quad (7)$$

In order to find the discretized values of the pressure field, eq. (7) is minimized under the constraint that the contact pressure is non-negative.

The approach can be extended to elasto-plastic contact by introducing an upper bound for the contact pressure and splitting the displacement into an elastic and a plastic part. Additional iterations are necessary in order to find the plastic and to correct the elastic displacements, cf. [3].

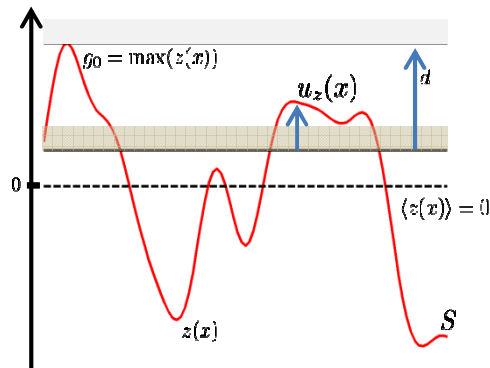


Figure 1: Contact between a flexible rough and a rigid flat surface.

3.2 Discretization of the random pressure field

Due to the randomness of the surface heights, the solution of the normal contact problem is a random pressure field. In principle, its properties could be determined by Monte Carlo simulation. To this end, the series representation of the surface roughness is truncated and sample surfaces are generated from samples of the random variables $\xi_j(\theta), j = 1, \dots, M$. Then, the elasto-plastic normal contact problem is solved for each sample surface to determine the pressure field. However, in order to describe precisely the cumulative density function of the pressure, a huge number of Monte Carlo simulations has to be performed. This is not suitable for large scale problems.

In the following, an approach based on regression and polynomial chaos expansion is introduced that permits to approximate the cumulative density function without drastically increasing the problem size. To simplify the explanation, we limit our approach to the determination of the pressure field at a given position \mathbf{x} which is a random variable $\tilde{p}_x(\theta)$. The approach can be easily extended to the determination of the complete pressure field. We will distinguish the pressure when contact occurs (i.e. when $\tilde{p}_x(\theta) > 0$, denoted $p_x(\theta)$) and probability of contact at a position \mathbf{x} which is given by $1 - \rho_{\tilde{p}}(0)$, where $\rho_{\tilde{p}}$ is the cumulative density function of $\tilde{p}_x(\theta)$.

By means of a polynomial chaos basis, the contact pressure can be expressed as the positive part of a polynomial expansion

$$p_x(\theta) = \left(\sum_{i=1}^P p_{x,i} \Gamma_i(\xi(\theta)) \right)^+ \quad (8)$$

or by expanding $\log(p_x(\theta))$:

$$\log(p_x(\theta)) = \sum_{i=1}^P \tilde{p}_{x,i} \Gamma_i(\xi(\theta)) \quad (9)$$

where $\Gamma_i(\xi(\theta)), \xi(\theta) = [\xi_i(\theta)]_{i=1, \dots, M}$, are multi-dimensional orthogonal polynomials. As

the functions $\Gamma_i(\xi(\theta))$ and the random variables $\xi(\theta)$ are known, the solution is fully determined by the coefficients $p_{x,i}$ and $\tilde{p}_{x,i}$, resp.

3.3 Determination of the expansion coefficients

The unknown expansion coefficients for the random pressure field are computed following a regression approach [4]. They are estimated from the minimization of the least square error between the polynomial representation and results $p_x^{(k)}$ for the pressure obtained for a set of K_t realizations of the random variables $\xi(\theta)$, denoted in the following by $\xi^{(k)}$, $k = 1, \dots, K_t$. E.g., the coefficients $p_{x,i}$, $i = 1, \dots, P$, are estimated by minimizing at each position \mathbf{x} :

$$\Delta p_x = \sum_{k=1}^{K_t} \left[p_x^{(k)} - \sum_{i=1}^P p_{x,i} \Gamma_i(\xi^{(k)}) \right]^2 \quad (10)$$

where $p_x^{(k)}$ is the pressure obtained by solving the normal contact problem for a smooth rigid plane and the rough surface defined by $z(\mathbf{x}, \xi^{(k)})$. Keeping only K realizations which induce a strictly positive pressure $p_x^{(k)}$, the coefficients read:

$$[p_{x,i}]_{i=1}^P = (\mathbf{\Gamma}^T \mathbf{\Gamma})^{-1} \mathbf{\Gamma}^T \mathbf{P}_x \quad (11)$$

where $\mathbf{\Gamma}$ is a $K \times P$ matrix such that $\Gamma_{ij} = \Gamma_j(\xi^{(i)})$ and \mathbf{P}_x is the vector containing the K contact pressures $p_x^{(k)}$, $k = 1, \dots, K$. To ensure the well-posedness of the problem, the number of realizations K has to be greater than P . Thus, for low penetration of the two surfaces, it might be necessary to generate a large number of samples. By selecting a Latin Hypercube Sampling scheme, few realizations are needed in order to estimate the unknown coefficients. From K/K_t , the probability of contact at position \mathbf{x} can be estimated, which completes the stochastic description of the contact pressure.

Figure 2 compares the distribution of the contact pressure obtained with Monte Carlo simulation, Latin Hypercube Sampling and polynomial chaos expansion with 165 expansion coefficients for a square shaped Gaussian surface with short correlation length (1/1000 of the edge length of the surface) leading to 101 coefficients in the Karhunen-Loève expansion. The penetration depth was the median of the surface heights. The two variants of the polynomial chaos expansion are nearly indistinguishable. Even for low probabilities, the polynomial chaos expansion matches well with the results obtained from Latin Hypercube Sampling.

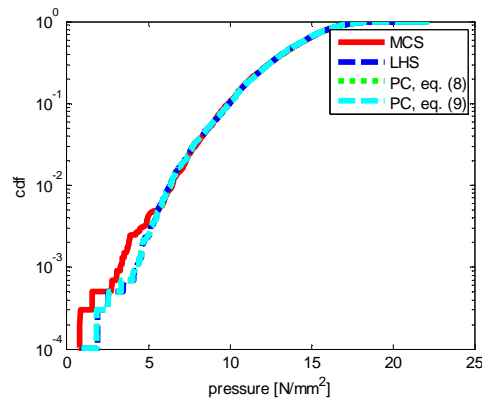


Figure 2: Cumulative distribution function for the contact pressure in the center of a Gaussian surface. Comparison of Monte Carlo simulation (MCS), Latin Hypercube Sampling (LHS), and polynomial chaos expansion (PC) according to eqs. (8) and (9), resp.

4 STOCHASTIC FRICTION COEFFICIENT

From the random pressure field, the Bowden-Tabor approach [5] for adhesive friction allows to determine a stochastic process for the friction coefficient μ . For a given test surface and under assumption of a shear dominated friction force, the friction coefficient is computed from $\mu = \frac{\tau_{max}}{N} A_c$, where τ_{max} is the shear strength of the material. The contact area A_c and the normal force N are obtained by averaging the pressure field on the test surface. The autocorrelation function of μ can be estimated by comparing the results for two test surfaces centered at different coordinates of the pressure field.

Figure 3 displays results for the mean value and the standard deviation of the friction coefficient for Gaussian surfaces as in the previous section but with dimension $25 \mu\text{m} \times 600 \mu\text{m}$ and different penetration depths d . Mean value, standard deviation and coefficient of variation decrease with increasing penetration depth, given as percentile of surface heights that are initially penetrated. The friction coefficient was found to be exponentially correlated with correlation length $250 \mu\text{m}$, independent of the penetration depth. The distribution of the friction coefficient deviates from a normal distribution, it is found to be right skewed and leptokurtic. When scaled to the interval (0,1) the friction coefficient follows a Beta(2.1,5)-distribution, independent of the penetration.

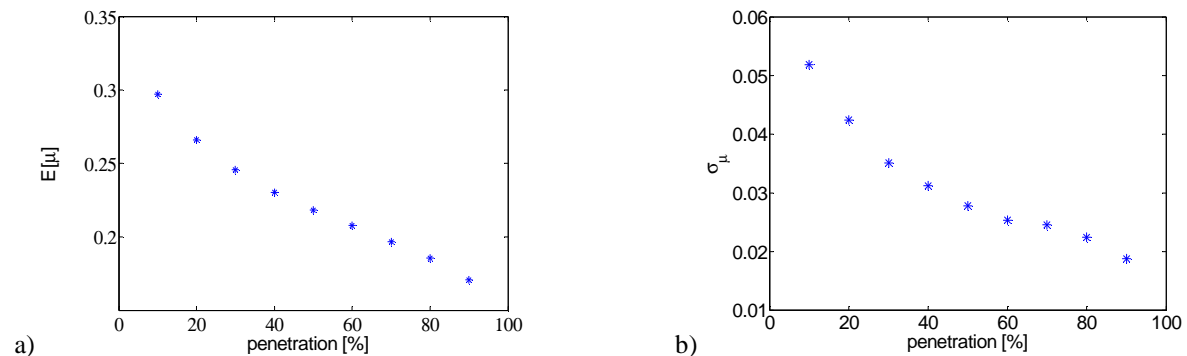


Figure 3: Mean value (a) and standard deviation (b) of the friction coefficient as function of the penetration.

5 STOCHASTIC FRICTION-INDUCED VIBRATIONS

The system under consideration consists of a mass m that moves on a belt, see Figure 4. The belt moves with constant velocity v_0 . The mass is attached to the surrounding by a spring (spring constant c) and a damper (damping constant d_k). It is externally excited by the harmonic force $Q\cos(\Omega t)$. Two different motion modes may occur:

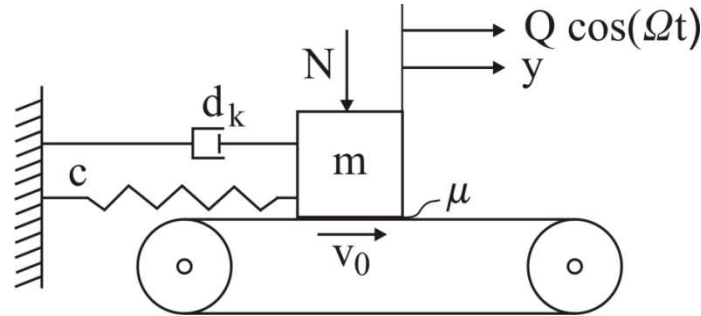


Figure 4: Friction induced vibrations of a mass on a belt.

the stick mode, where the mass sticks to the belt and the slip mode, where the mass slips due to the restoring force. The conditions for the stick mode are

$$\dot{x} = v_0 \text{ and } |F_{Rst}| \geq |cy + d_k\dot{y} - Q\cos(\Omega t)|. \quad (12)$$

In slip mode, the friction force $F_R = \mu(v_{rel})N\text{sign}(v_{rel})$ changes its sign according to the direction of the relative velocity v_{rel} between mass and belt. The friction coefficient $\mu(v_{rel})$ is represented by a deterministic and a stochastic part: $\mu = \mu_D + \mu_S$. The deterministic part is described by a Stribeck law

$$\mu_D = \frac{\mu_{fit}(d)}{1 + 1.42|v_{rel}|} + 0.4 - \mu_{fit}(d) + 0.01v_{rel}^2 \quad (13)$$

with $\mu_{fit}(d)$ obtained from the mean value curve, Figure 3 a). The stochastic part is modeled by a stochastic process that is generated from the spectral representation. Realizations of the stochastic process are generated, transformed from space to time domain and the equation of motion is integrated by a Runge-Kutta-Fehlberg method. For self-excitation, a natural frequency of $\omega = 316 \frac{1}{s}$, a damping coefficient of 0.17, a velocity of the belt of $\frac{v_0}{\omega} = 0.003$, and a normal force of 2.5 kN, Figure 5 displays the limit cycle for the dimensionless displacement X_1 and velocity X_2 of the mass and the empirical probability density function for the reattachment point X_{gh} of the stick-slip limit cycle. By comparison with the normal probability density function, it can be clearly seen that also the reattachment point is nonnormally distributed. Figure 5 c) displays the difference $M_{diff} = M_d - E[M_S]$ between the number of limit cycles for the deterministic system ($\mu_S = 0$) and the mean number of limit cycles of the stochastic system in the same amount of time for different values of the damping coefficient. While for the deterministic system, there is a sharp limit for the damping coefficient where the limit cycle ceases to exist, there is a range of values for the damping coefficient where the stochastic system can still move on the limit cycle.

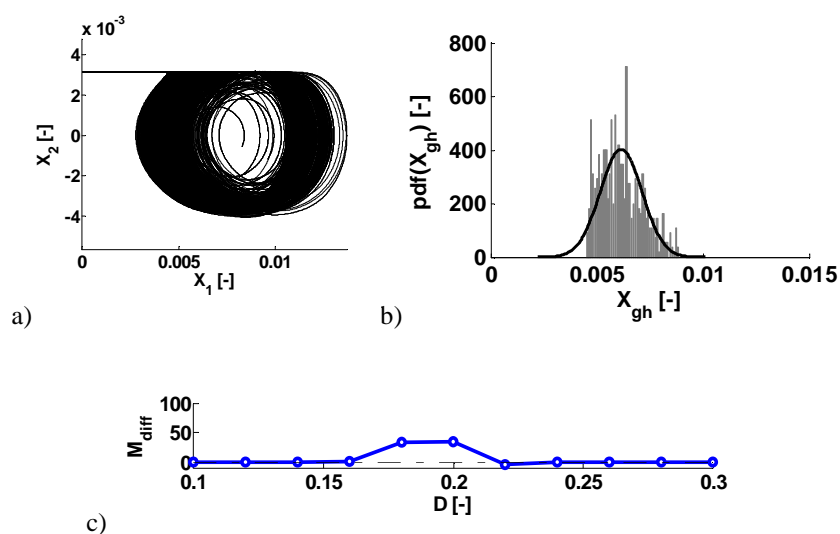


Figure 5: Limit cycle (a), histogram for the reattachment point (b), and difference between the number of limitcycles for the deterministic and the stochastic system (c).

6 CONCLUSIONS

A method has been developed that models uncertainties due to surface roughness and studies its influence on the friction coefficient and on friction induced vibrations. The surface heights of the rough surface are described by a truncated Karhunen-Loève expansion. The resulting pressure field under normal contact is represented by a polynomial chaos expansion and the probability of contact has been computed. Finally, the friction coefficient is modeled as a stochastic process whose properties are obtained following the Bowden-Tabor approach. It could be shown that the statistical characteristics of the friction coefficient depend on the contact pressure and are non-normal. For friction induced vibrations, the stochastic nature of the friction coefficient influences the stick-slip limit cycle. This effect can be investigated with a simple model of a mass on a belt by studying the properties of the limit cycle and comparing the results to the deterministic case.

BIBLIOGRAFIA

- [1] O. Ahmad, *Stochastic representation and analysis of rough surface topography by random fields and integral geometry - Application to the UHMWPE cup involved in total hip arthroplasty*, Doctoral Thesis, Ecole Nationale Supérieure des Mines de Saint-Etienne (2013).
- [2] M. Ausloos and D.H. Berman, "A multivariate Weierstrass-Mandelbrot function", *Proc. R. Soc. Lond. A*, **400**, 331-350 (1985).
- [3] K. Willner, "Elasto-plastic normal contact of three-dimensional fractal surfaces using halfspace theory", *ASME Journal of Tribology*, **126**, 28-33 (2004).
- [4] G. Blatman and B. Sudret, "Sparse polynomial chaos expansions and adaptive stochastic finite elements using a regression approach", *Comptes Rendus Mécanique*, **336**, 518-523 (2008).
- [5] F.P. Bowden and D. Tabor, *The friction and lubrication of solids*, Clarendon Press, Oxford (1950).